Colour centres, dislocations and colloids in ion-implanted LiF and LiF(Mg)

1995 J. Phys.: Condens. Matter 7 3211

(http://iopscience.iop.org/0953-8984/7/17/005)

J. Phys.: Condens. Matter 7 (1995) 3211–3226. Printed in the UK

Colour centres, dislocations and colloids in ion-implanted LiF and LiF(Mg)

A T Davidson†, J D Comins‡, A M J Raphuthi†‖, A G Kozakiewicz†, E J Sendezera† and T E Derry§

† Physics Department, University of Zululand, KwaDlangezwa 3886, South Africa
‡ Department of Physics, University of the Witwatersrand, Johannesburg 2050, South Africa
§ Schonland Research Centre for Nuclear Sciences, University of the Witwatersrand, Johannesburg 2050, South Africa

Received 28 September 1994, in final form 23 December 1994

Abstract. Pure and magnesium-doped LiF crystals have been implanted with mainly magnesium and argon ions of 100 keV energy. Fluences were in the range of 6×10^{15}–1×10^{17} ions cm^{-2}. Changes in optical absorption during thermal annealing are reported. The magnesium colloid band at 280 nm and the lithium colloid band at 520 nm are identified. Some cases of anomalous colloid growth are observed. Hidden structural factors such as dislocations are thought to produce this anomalous annealing behaviour. Magnesium colloids develop in doped crystals after the implantation of rare gas ions. The responsible mechanism is thought to involve the interaction of F centres with impurity–vacancy (IV) dipoles. We find that the dopant has little effect on the concentration of F and F_2 colour centres or on their thermal stability in ion-implanted samples.

1. Introduction

This paper concerns optical effects in ion-implanted LiF crystals observed during the course of thermal annealing. Ion implantation introduces defects at large concentrations in a thin region near the surface of the crystal, determined by the range of penetration of the ions. Although vacancies and interstitial ions might be expected to occur by direct displacement on both sublattices in ion-implanted samples, there is little evidence of this in alkali halide crystals, which do not amorphize easily. Rather defects are produced on the anion sublattice by the excitonic mechanism, which is an efficient process of electronic excitation in ionic crystals. In the case of alkali halides, the primary defects are F and H centres which, under the appropriate conditions, can aggregate to form complexes (see for example Hobbs (1975), Townsend (1987) and Comins *et al* (1988)). Thermal annealing subsequent to implantation will alter the inventory of defects and also the spatial distribution of the implanted ions. The present work investigates crystals implanted with mainly, but not exclusively, magnesium and argon ions. Magnesium-doped crystals are also included. These contain charge-compensating cation vacancies and are of interest for their thermoluminescent properties (Mayhugh *et al* 1970, McKeever 1985).

Colouration of LiF crystals by ions in the energy range 100 keV–2 MeV has been reported previously by Davenas *et al* (1973), Afonso *et al* (1985) and Abu-Hassan and Townsend (1986). H^+, He^+, N^+, B^+, O^+, Ne^+ and the alkali ions Li^+, Na^+ and K^+ were investigated. These and our own studies using Na^+, Mg^+, Ne^+ and Ar^+ ions (Davidson

‖ Now at Clark Atlanta University, USA.

0953-8984/95/173211+16$19.50

et al 1985, 1986) show that colouration is due to F and F aggregate centres formed in the implanted region. At sufficiently large fluences there may be extra colouration due to small metallic particles usually referred to as colloids. Annealing experiments undertaken by the above workers generally report the growth of prominent absorption bands in crystals implanted with metallic ions. This is also attributed to colloids originating from the implanted ions. Intrinsic lithium colloids can also form and this aspect will be discussed in some detail in this paper.

2. Experimental procedure

Pure and magnesium-doped plates of thickness 1 mm were obtained from BDH (Merck) in the United Kingdom. The doped plates contained 0.5 wt% of MgF_2, which corresponds to 2000 ppm of Mg. Square specimens of side 6 mm were cut from the plates using a diamond wire saw. Ion implantations with 100 keV ions were performed at the Schonland Research Centre for Nuclear Sciences at the University of the Witwatersrand. Beam currents were in the range 2–8 μA cm^{-2} at fluences between 6×10^{15} and 1×10^{17} ions cm^{-2}. Implantations were carried out with crystals initially at ambient temperature with no active cooling during implantation. Under these conditions, a significant temperature rise of the crystal surface will occur, especially at the larger beam currents. An indication of the temperatures involved is given in our work on MgF_2 (Davidson *et al* 1993). The penetration depth of 100 keV ions in LiF is estimated to be about 0.08 μm for argon ions and about 0.14 μm for magnesium ions. Further details of the implantation procedure have been given previously (Davidson *et al* 1985).

Optical absorption spectra were measured at wavelengths between 200 nm and 700 nm using a Beckman Du-8 spectrophotometer. Crystals were isochronally annealed in air in a horizontal tube furnace. Annealing proceeded in nominal steps of 50 °C starting at a temperature of 50 °C. The annealing period at a given temperature was usually 30 min. After each annealing step, the crystal was rapidly cooled to ambient temperature, where the absorption spectrum was measured. Some clarification of the figures presented in this paper may be helpful. When dealing with annealing measurements, the curve a shows the absorption spectrum following ion implantation. All implanted crystals were subjected to the same sequential annealing steps described above, but only selected spectra are reproduced here. These were chosen to demonstrate significant changes in the absorption spectrum of the crystal concerned, and curves b, c, d etc in the various figures are not necessarily indicative of the same annealing temperature. We have extracted growth curves in figure 1(b) and figure 8(b) without using computerized fitting procedures. Peak absorbance levels are influenced by overlapping bands and with comparatively few data points are merely indicative of general trends produced by annealing. Table 1 provides a summary of ion types and fluence levels investigated in detail in this paper. We identify the main defect centres in each case and list the figures and parts of the text where results pertaining to a given sample can be found.

3. Results

3.1. Magnesium ion implantation of pure samples

Figure 1(a) shows absorbance spectra observed at different stages during an isochronal anneal of a pure crystal implanted with 6.0×10^{15} ions cm^{-2}. F (4.96 eV), F_2 (2.80 eV)

Table 1. *Defect centres observed in the present investigation of ion-implanted LiF crystals. Full shading indicates centres present in as-implanted samples. Partial shading indicates* centres produced by subsequent annealing. Colloids are indicated by squares. Triangles indicate remanent absorption at high annealing temperatures attributed to colloids.

	Z_3?	F	Mg *colloid*	Z_2?	F_3	F_2	Li *colloid*	Li *colloid*	Text and figure index
	5.74 *216*	4.96 *250*	4.43 *280*	3.87 *320*	3.32 *377*	2.80 *443*	3.58 *346*	2.38 (eV) *520 (nm)*	
a) Magnesium ions (cm^{-2})									
i) LiF (pure)									
6×10^{15}		●	▨		●	●		▲	3.1 1a, 1b, 9a
1×10^{16} (a)	◐	●	▨	◐		●		▲	3.1 2, 9a
(b) anomalous		●				●	▲	▲	
8.7×10^{16}			■				▨	▨	3.3 6
ii) LiF (2000 ppm Mg)									3.1 3, 9a
1×10^{16}	◐	●	▨	◐		●			
8.7×10^{16}			■						3.4
									3.4
b) Rare gas ions (cm^{-2})									
i) LiF (pure)									
1×10^{16} (Ar)		●				●			
1×10^{17} (Ar)		●				●	▨	■	3.2 4
1×10^{17} (Ne)		●			●	●			3.2 5
ii) LiF (2000 ppm Mg)									3.4 7
1×10^{17} (Ar)		●	▨			●			
1×10^{17} (Ne)		●				●		■	3.4 8a, 8b, 9b
									3.4 7

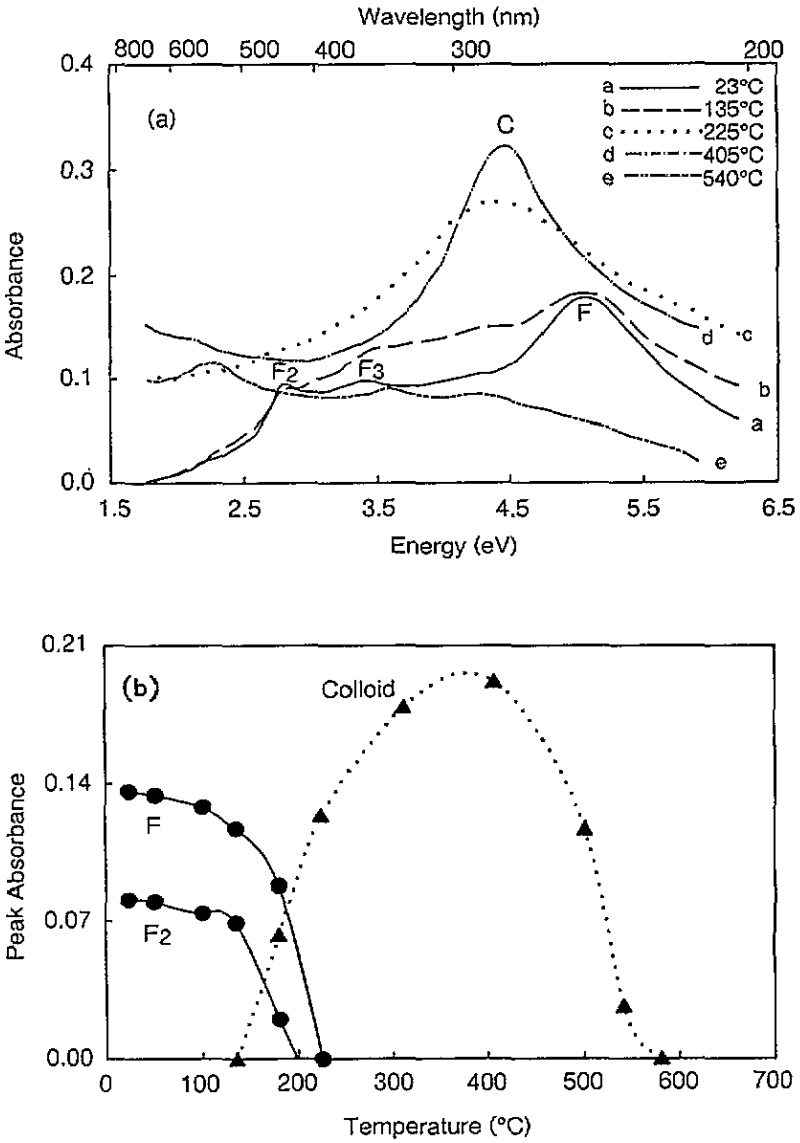

Figure 1. (a) The annealing behaviour of a LiF crystal after implantation with 6×10^{15} magnesium ions cm^{-2} at ambient temperature without active cooling. The beam current was 3 $\mu A\ cm^{-2}$. The curves show absorbance spectra during stages of an isochronal anneal. (b) The temperature dependence of the main absorption bands shown in (a).

and F_3 (3.32 eV) bands are present initially. As annealing proceeds to 400 °C, a broad band *C* (280 nm, 4.43 eV) becomes a prominent feature of the absorption spectrum. Band *C*, which we identify as a magnesium colloid band for reasons to be discussed later, disappears after annealing to 540 °C. During the high-temperature stage of the anneal near 540 °C, the implanted region assumes a violet colour. This may be associated with a band near 2.3 eV in the absorption spectrum at this temperature. In figure 1(b) we show the temperature dependence of the main absorption bands appearing in figure 1(a).

The annealing behaviour of a crystal implanted with 1.0×10^{16} ions cm^{-2} is shown in

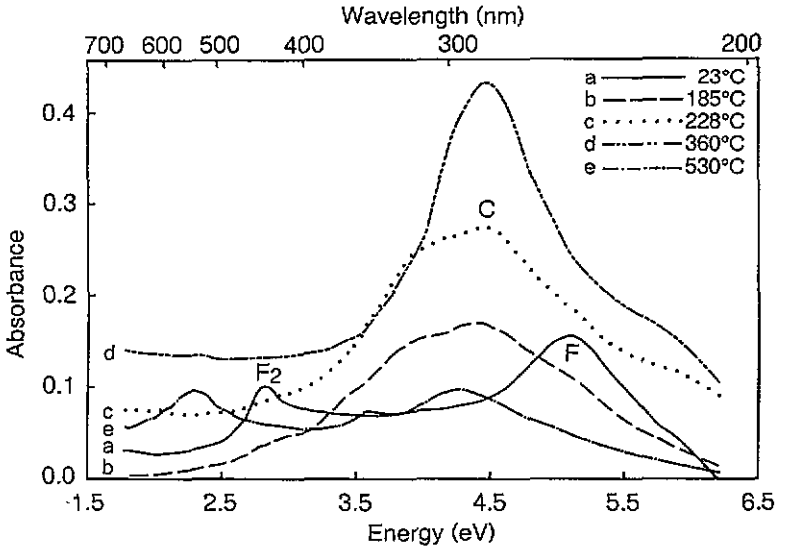

Figure 2. The annealing behaviour of a LiF crystal after implantation with 1×10^{16} magnesium ions cm^{-2} at ambient temperature without active cooling. The beam current was 3 $\mu A\ cm^{-2}$. The curves show absorbance spectra during stages of an isochronal anneal.

figure 2. Colour centre bands anneal out by about 180 °C as before and this is accompanied by increased absorption in the 290 nm wavelength region. After the 185 °C anneal, new bands are resolved at 280 nm (4.43 eV) and at 320 nm (3.87 eV) in the absorption spectrum. After the 270 °C anneal, the colloid band at 280 nm is dominant. At the next annealing stage (320 °C), a weak shoulder appears near 216 nm on the high-energy side of the colloid band. After further annealing to a temperature of 530 °C, a distinct violet colouration of the implanted region occurs, similar to that mentioned previously. This is associated with bands near 543 nm (2.28 eV) and 346 nm (3.58 eV) as can be seen in curve e of figure 2.

Figure 3 shows the annealing behaviour of a crystal implanted with 8.7×10^{16} ions cm^{-2}. A magnesium colloid band has already formed during implantation and F aggregate concentrations are small. Subsequent annealing enhances this band, with the main growth occurring at temperatures between 230 °C and 360 °C. The colloid band grows at similar temperatures in samples implanted with lower doses of magnesium ions, as can be seen in figure 1(b).

3.2. Argon ion implantation of pure samples

Effects observed when annealing argon-ion-implanted crystals are shown in figures 4 and 5 for fluences of 1×10^{16} and 1×10^{17} ions cm^{-2} respectively. A feature of these data is that the F and F_2 bands remain observable to higher temperatures in comparison with magnesium-implanted crystals. In figure 5, an extra band is present near 520 nm (2.38 eV) in the as-implanted crystal. Annealing enhances this band and also produces a new band near 365 nm (3.40 eV). We have suggested previously that the 520 nm band is associated with an intrinsic lithium colloid (Davidson *et al* 1986). Annealing the lower-dose (1×10^{16} argon ions cm^{-2}) crystal shown in figure 4 gradually removes the F and F_2 bands at temperatures between 150 °C and 320 °C and no new bands are produced. This sample showed significant absorption at shorter wavelengths. We have seen this in a few other cases as well but have not investigated the effect further.

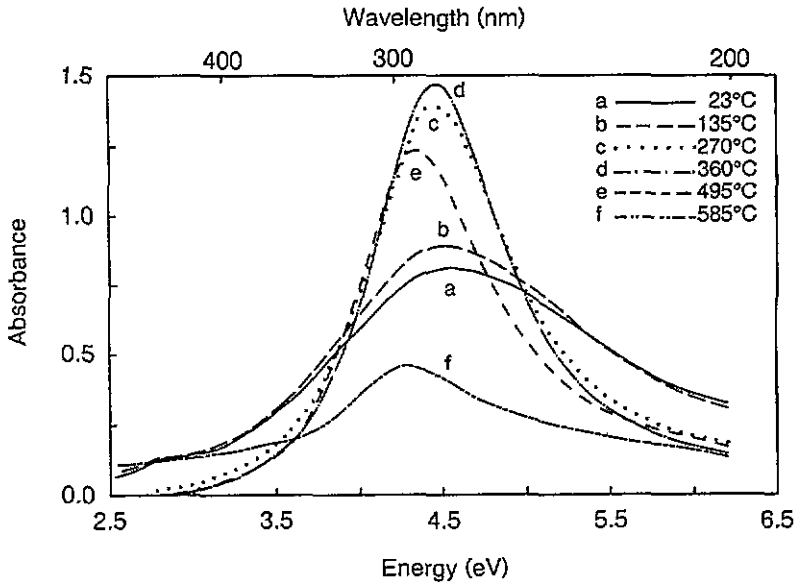

Figure 3. The annealing behaviour of a LiF crystal after implantation with 8.7×10^{16} magnesium ions cm^{-2} at ambient temperature without active cooling. The beam current was 3 $\mu A\ cm^{-2}$. The curves show absorbance spectra during stages of an isochronal anneal.

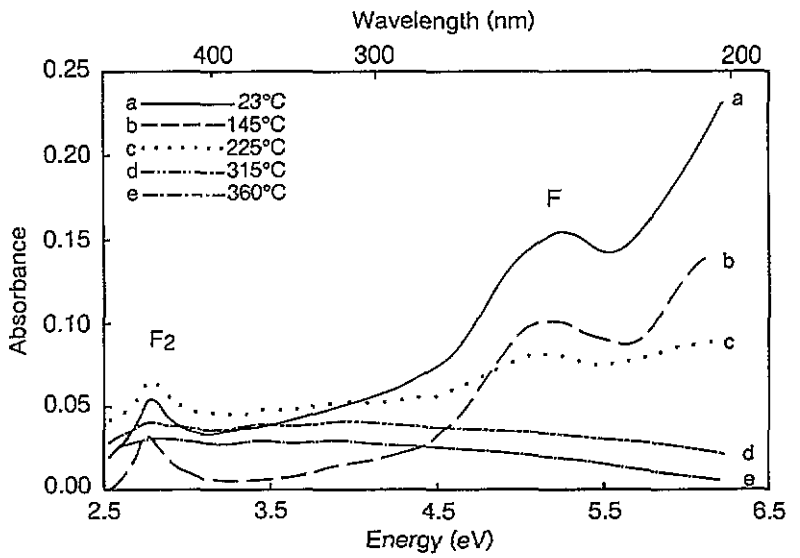

Figure 4. The annealing behaviour of a LiF crystal after implantation with 1×10^{16} argon ions cm^{-2} at ambient temperature without active cooling. The beam current was 8 $\mu A\ cm^{-2}$. The curves show absorbance spectra during stages of an isochronal anneal.

3.3. Anomalous results with magnesium- and sodium-ion-implanted samples

Occasionally we observe deviant annealing behaviour in pure crystals implanted with magnesium or sodium ions at fluences of 1×10^{16} ions cm^{-2}. An example is shown in

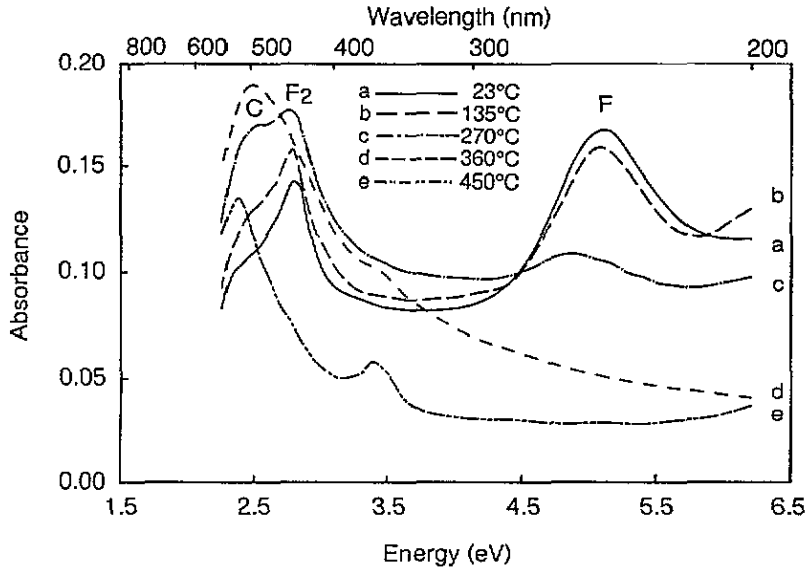

Figure 5. The annealing behaviour of a LiF crystal after implantation with 1×10^{17} argon ions cm^{-2} at ambient temperature without active cooling. The beam current was 8 μA cm^{-2}. The curves show absorbance spectra during stages of an isochronal anneal.

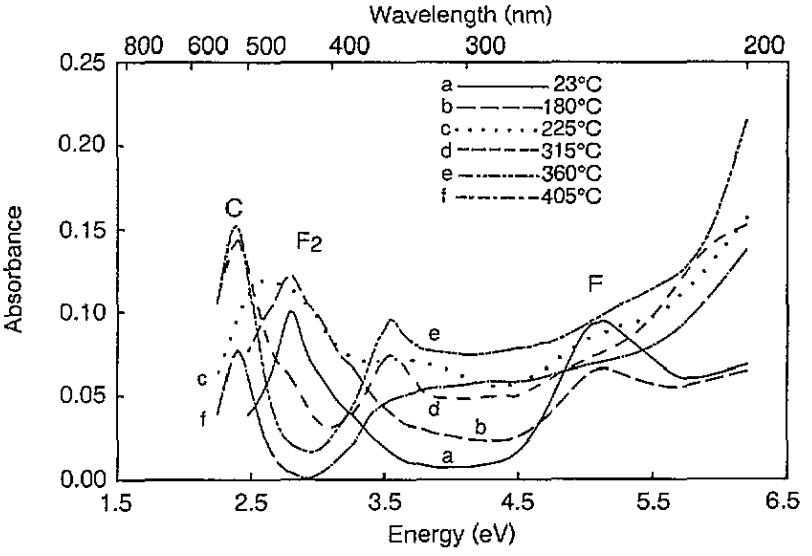

Figure 6. Anomalous annealing behaviour of a LiF crystal after implantation with 1×10^{16} magnesium ions cm^{-2} at ambient temperature without active cooling. The beam current was 3 μA cm^{-2}. The curves show absorbance spectra during stages of an isochronal anneal. Contrasting behaviour is shown in figure 2.

figure 6 for a magnesium-implanted crystal. In contrast to the behaviour of a similar crystal in figure 2, the crystal in figure 6 shows behaviour indicative of lithium colloid formation.

In other words the annealing behaviour of the magnesium-ion-implanted crystal shown in figure 6 is almost identical with that of the argon-ion-implanted crystal shown in figure 5. It is interesting that similar behaviour to that shown in figure 6 was reported by Davenas *et al* (1973) when annealing a LiF crystal implanted with 1×10^{16} sodium ions cm^{-2}. The anomalous behaviour reported here is thus a confirmed effect requiring explanation. We note that the crystal showing intrinsic behaviour on annealing (figure 6) has comparatively little absorption in the region between the F and F_2 bands prior to annealing, in contrast to the crystal shown in figure 2.

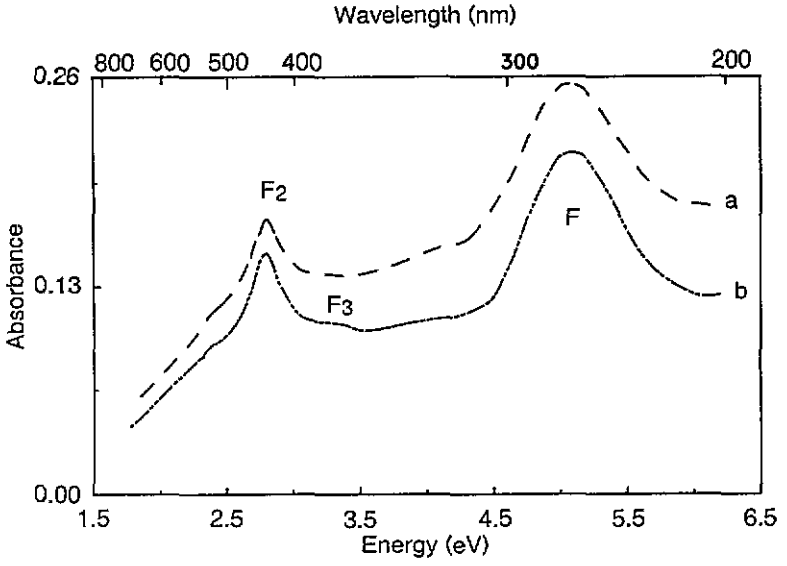

Figure 7. Absorbance against photon energy between 2.0 and 6.2 eV for pure and magnesium-doped (2000 ppm) crystals of LiF implanted with the same fluence of neon ions (100 keV, 7.5 μA cm^{-2}, 1×10^{17} ions cm^{-2}) at ambient temperature without active cooling: a, LiF(Mg); b, LiF (pure).

3.4. Magnesium-doped samples

In general, doping does not have a strong influence on the colouration of crystals implanted with 100 keV ions. This observation is based on implantations with Mg^+, Ar^+ and Ne^+ ions under comparable conditions. Absorption spectra of pure and doped crystals implanted with 1×10^{17} neon ions cm^{-2} are compared in figure 7. F and F_2 absorbance levels are about 10% smaller in the case of the doped crystal. A reduction of about 20% was observed for doped crystals implanted with 1×10^{16} magnesium ions cm^{-2}.

However doped crystals do show different colloid growth on annealing. Considering firstly crystals implanted with rare gas ions, figure 8(a) shows absorption spectra at stages of an isochronal anneal of a doped crystal implanted with 1×10^{17} argon ions cm^{-2}. The temperature dependence of the absorption bands appearing in figure 8(a) is given in figure 8(b). It can be seen that both the F and the F_2 bands disappear by 315 °C. This is similar to the annealing behaviour of a pure crystal shown in figure 5. Looking at the colloid bands in figure 8(a) for a doped crystal, we see that a band (lithium colloid) is

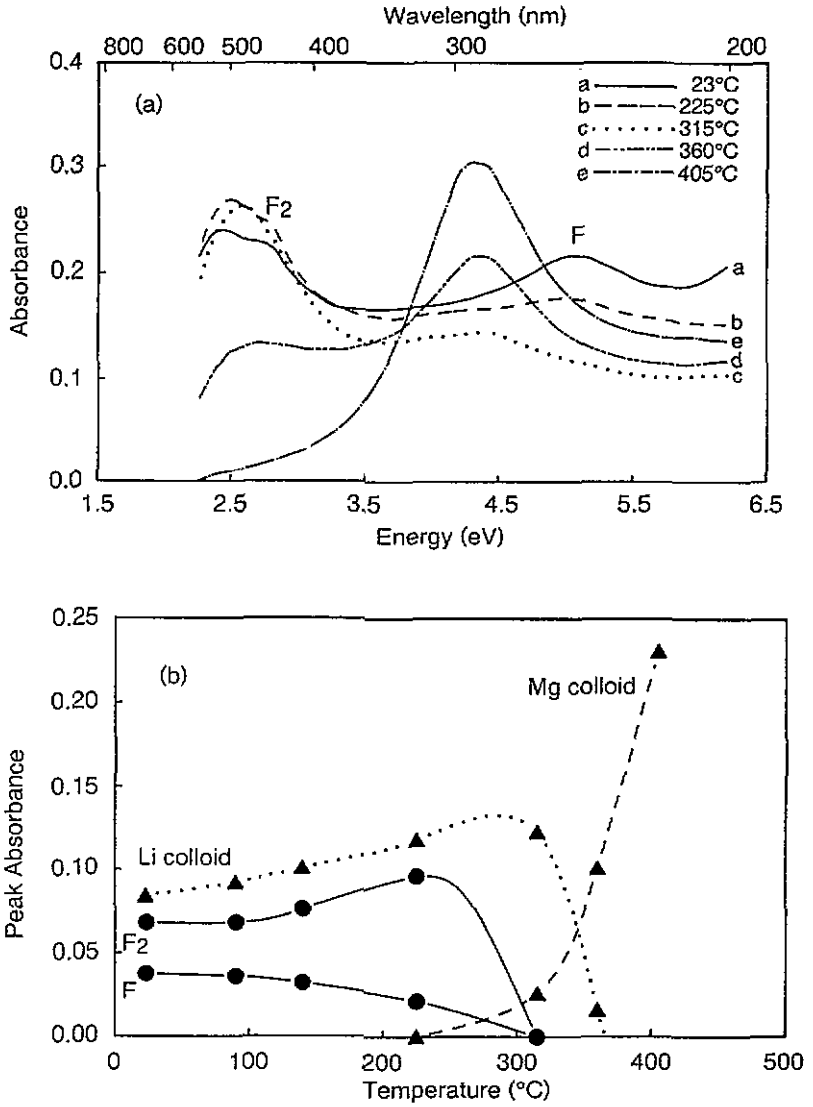

Figure 8. (a) The annealing behaviour of a magnesium-doped (2000 ppm) LiF crystal after implantation with 1×10^{17} argon ions cm^{-2} (100 keV, 2.5 μA cm^{-2}) at ambient temperature without active cooling. The curves show absorbance spectra during stages of an isochronal anneal. Contrasting behaviour of a pure crystal is shown in figure 5. (b) The temperature dependence of the absorption bands shown in (a).

present at 520 nm initially but gives way to a band (magnesium colloid) near 280 nm as annealing proceeds. This behaviour is quite different to that of the pure crystal, shown in figure 5. Annealing a doped crystal implanted with 1×10^{16} xenon ions cm^{-2} also produced a magnesium colloid band near 283 nm (4.38 eV) at a temperature of 400 °C, as did a crystal doped with a lower concentration (100 ppm) of magnesium and implanted with 1×10^{16} argon ions cm^{-2}. In the latter case, the magnesium colloid band was very small but occurred at similar annealing temperatures as before.

Considering next doped crystals implanted with magnesium ions, we have annealed a

crystal implanted with 1×10^{16} magnesium ions cm^{-2}. The behaviour is similar in some ways to the pure crystal in figure 2. The F and F_2 bands both disappeared after the 230 °C anneal in the doped crystal. The corresponding annealing temperature for the pure crystal was 185 °C. After the 230 °C anneal the magnesium colloid band at 280 nm was prominent in the doped crystal. This situation pertained until 320 °C when a new band emerged near 310 nm. This band may have the same origins as the 320 nm band in figure 2, thus it appears at a somewhat higher temperature in the doped crystal. By 360 °C, the band at 310 nm was dominant with the 280 nm band being a shoulder. On further annealing to higher temperatures, the peak position moved back to 280 nm and it finally disappeared at about 570 °C. As in the pure crystal, a small band appeared near 216 nm after the 320 °C anneal and was present at higher temperatures as well. We did not observe violet colouration in the doped crystal after annealing at high temperatures.

We have also annealed a crystal implanted with a large dose (8.7×10^{16} cm^{-2}) of magnesium ions. Results were similar to those for the pure crystal shown in figure 3. However, if we compare the optical density (OD) of the magnesium colloid bands at an annealing temperature of 360 °C where both have near-maximum values, we find that the colloid band is more prominent in the pure ($OD_{max} = 1.37$) than in the doped ($OD_{max} = 0.81$) crystal.

3.5. Intrinsic and extrinsic magnesium colloids

In the previous sections we indicated that both magnesium-doped and magnesium-implanted crystals can give rise to magnesium colloids when suitable annealing procedures are followed. It is of interest to compare the shape of the prominent colloid bands in the two cases. Figure 9(a) is for pure crystals implanted with magnesium ions at fluences in the range 6.0×10^{15}–8.7×10^{16} ions cm^{-2} and annealed to 360 °C and figure 9(b) is for doped crystals implanted with rare gas ions in the range 1×10^{16}–1×10^{17} ions cm^{-2} and also annealed at 360 °C. The colloid band occurs at slightly higher energy in the implanted crystals (278.3 nm, 4.45 eV) than in the doped crystals (286.0 nm, 4.33 eV). The half width of the bands is similar. Good peak agreement in the two cases supports our assignment of the band near 280 nm to a magnesium colloid (see table 2). We note the interesting circumstances leading to the formation of the intrinsic magnesium colloid in doped crystals. It has similarities with the gettering process used in the purification of semiconductor devices (see for example the article by Lecrosnier (1983)).

4. Discussion

4.1. Colour centres

It is apparent that magnesium doping does not have a large influence on the concentration of F and F_2 colour centres in as-implanted crystals. Neither is their thermal stability much affected by the presence of the dopant. The latter behaviour is in sharp contrast to our crystals coloured by γ-irradiation. However we find that F and F_2 colour centres remain observable to signficantly higher annealing temperatures in argon-ion-implanted crystals than in magnesium-ion-implanted crystals, irrespective of doping. This suggests that the thermal stability of colour centres is related to the type of ion implanted or to effects introduced during ion implantation. Two processes have been suggested for the disappearance of F centres. One is their recombination with complementary halogen interstitials with accompanying luminescence and the other is their aggregation to form

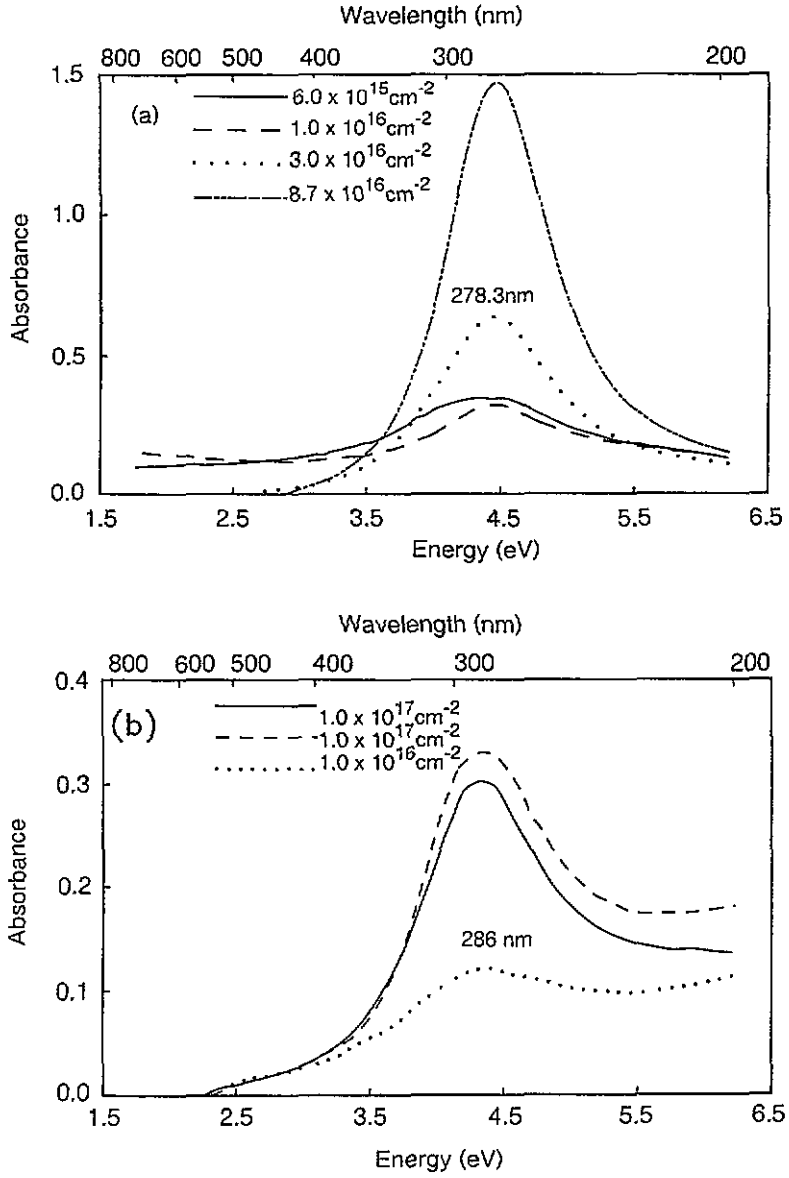

Figure 9. (a) The magnesium colloid band in nominally pure LiF crystals. Crystals were implanted with magnesium ions at ambient temperature without active cooling. Absorption spectra are shown for different crystals after the 360 °C stage of an isochronal anneal. Fluence levels are indicated in the figure. (b) The magnesium colloid band in magnesium-doped (2000 ppm) LiF crystals. Crystals were implanted with rare gas ions at ambient temperature without active cooling. Absorption spectra are shown for different crystals after the 360 °C stage of an isochronal anneal. Fluence levels are indicated in the figure. The dotted curve is for xenon ions and the other curves are for argon ions.

alkali metal colloids. It may not be possible to decide their relative importance at this stage. This is because the annealing behaviour of the V_3 band, which is representative of halogen interstitials, is not known in sufficient detail in lithium fluoride as it is located in

Table 2. The peak energy (in electronvolt) of colloid bands observed in our ion-implanted LiF crystals. The predicted peak energy of the colloid band ($\hbar\omega_c$) depends on the plasmon energy ($\hbar\omega_p$) and is calculated using $\hbar\omega_c = \hbar\omega_p(1 + 2n^2)^{-1/2}$ (Doyle 1958). n is the refractive index of LiF at the appropriate frequency, ω_c (values of refractive index in the range 1.44–1.39 from Gray (1972)). Na and Al colloids were produced in as-implanted crystals with no annealing procedures. Na, Davidson *et al* (1985); Al, Davidson *et al* (unpublished).

	^{11}Na	^{3}Li	^{12}Mg	^{13}Al
Plasmon energy[a]	5.71	7.12	10.6	15.3
$(\hbar\omega_c)_{observed}$	2.74	2.38[b]	4.45[c]	6.11
		2.79[d]	4.33[e]	
		3.40[f]		
$(\hbar\omega_c)_{predicted}$	2.58	3.22	4.74	6.75

[a] Values of plasmon energy (in electronvolt) from Kittel (1976).
[b] Intrinsic colloid in an Ar^+-implanted crystal.
[c] Extrinsic colloid in an Mg^+-implanted crystal.
[d] Extrinsic colloid in an Li^+-implanted crystal, from Davenas *et al* (1973).
[e] Intrinsic colloid in an Mg-doped crystal.
[f] Side band attributed to anisotropic colloid.

the vacuum ultraviolet spectral region. Davidson *et al* (1985) have reported some annealing measurements in this region.

The effect shown in figure 1 and in figure 8 whereby the growth of colloid bands occurs at the expense of the F band and smaller F aggregates is characteristic of the annealing behaviour of most of our ion-implanted crystals. Thus it appears that the presence of F centres in large concentrations favours the growth of colloids on annealing. The colloid bands seen in as-implanted crystals at large fluences probably also result from the heating effects of the ion beam and the consequent annealing of F centres during implantation. Electrons released from F centres are thought to play a key role in the following cases: intrinsic lithium colloids, which form in pure crystals implanted with rare gas ions, and intrinsic magnesium colloids, which form in doped crystals implanted with rare gas ions. Both are thought to involve the donation of F centre electrons to cations to produce neutral metal particles. In magnesium-doped crystals, two F centres are needed to neutralize an Mg^{2+} ion. The associated vacancies, comprising a cation vacancy originating from IV dipoles and anion vacancies from F centres, provide the necessary void space for the metallic particles. A diagram showing the steps involved in the formation of intrinsic magnesium colloids is given in figure 10.

In the case of crystals implanted with magnesium ions at the lower fluences, changes produced by annealing are more complex, with extra absorption bands being produced and, in a few crystals, anomalous annealing behaviour being observed. Referring to figure 2, new bands evolve near 280 nm and 320 nm in a pure crystal implanted with 1×10^{16} magnesium ions cm^{-2}. A weak band develops later near 216 nm at higher annealing temperatures. Bands at similar wavelengths are known from investigations of magnesium-doped crystals coloured by x-irradiation and have been associated with thermoluminescence (see the article by Crittenden *et al* (1974)). Their origin is uncertain. On the one hand they may be perturbed F centres associated with the divalent impurity as proposed by Kos and Nink (1977, 1979) and Agulló-López *et al* (1982). On the other hand, Landreth and McKeever (1985) associate a band at 310 nm with a cluster (trimer) of magnesium vacancy dipoles. Bands at 280 nm and 217 nm are thought by them to be magnesium related and not Z type in origin. Of the bands induced by annealing in figure 2, the 320 nm band is prominent initially together with the magnesium colloid band at 280 nm. Theoretical

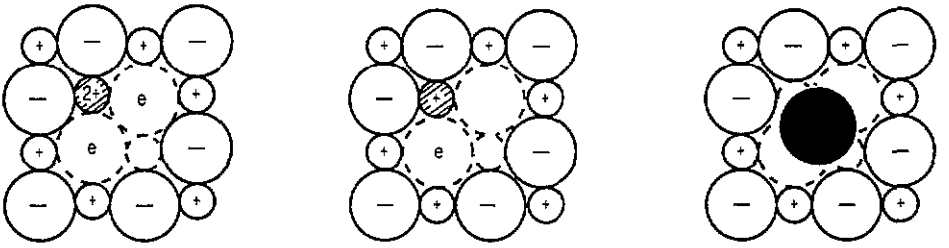

Figure 10. A two-dimensional representation of the conversion of an IV dipole in a magnesium-doped crystal of LiF to a magnesium atom with the loss of two F centres. The dashed circles indicate vacancies. F centres are represented by dashed circles enclosing an e symbol. The shaded circle is a magnesium ion being converted and the dark circle is a magnesium atom, Mg^0.

calculations by Shluger *et al* (1988) attribute absorption in the 310 nm region to the Mg^+–V_aV_c centre. This is consistent with our model for colloid development mentioned earlier. We might have expected to see this band while annealing doped crystals implanted with argon ions. As can be seen in figure 8, this was not the case and the intermediate step of figure 10 is absent here. Another possible contributor to absorption at 320 nm, which at first sight does not involve impurities, is the R_1 centre, absorbing at 306 nm. This is one of two absorption bands associated with F_3 complexes (Beall Fowler 1968). The other band (R_2) occurs at 377 nm and is resolved in some of our ion-implanted crystals prior to annealing (see figures 1 and 7).

4.2. Magnesium colloids

The present experiments have produced magnesium colloids by two different methods, firstly by implanting magnesium ions and secondly in crystals containing a significant amount of magnesium as a dopant. In the latter case, the doped crystals are implanted with rare gas ions prior to annealing. If this is not done, the colloid band does not form on annealing doped crystals. The magnesium colloid band is located near 280 nm in both cases. Surprisingly, if magnesium-doped crystals are implanted with magnesium ions, the colloid band is reduced in size when compared with pure crystals implanted and annealed under the same conditions. This is perhaps a further indication that F centres participate in the formation of colloids if we suppose that the number of available F centres is reduced by the presence of the dopant. The processes leading to the development of extrinsic magnesium colloids are still rather uncertain, however. The significant growth of the colloid band apparent in figure 1(b) after colour centres have annealed may indicate that the mobility of magnesium atoms is a factor in the development of extrinsic colloids.

We have already noted that the aggregation of magnesium impurities occurring in figure 8 has similarities with the gettering process in semiconductors. Here gettering refers to the removal of unwanted metallic impurities from active regions of a device. Thus if a crystal such as silicon is heavily implanted, it is reported that fast-diffusing atoms from the bulk become trapped at defects in the implanted region. In the present case of doped LiF crystals, it appears that the essential step of argon ion implantation prior to annealing serves to generate F centres, which then interact with IV aggregates and neutralize the impurity ions, which develop into magnesium colloids.

4.3. Lithium colloids

An interesting effect in pure crystals is the type of colloid produced by implanting argon ions at large fluences of about 1×10^{17} ions cm^{-2}. The band is located near 520 nm (2.38 eV) as shown in figure 5. We think that it is due to lithium derived from the target crystal, for reasons to be discussed in the next paragraph. There is evidence from our results that the lithium colloid sometimes becomes non-spherical or even platelike in view of the second absorption band near 365 nm (3.40 eV), which is produced together with the colloid band in annealing experiments. Theories of plasmon oscillations in non-spherical metal particles based on the Mie theory predict such doubling effects in optical absorption spectra. The separation of the component bands is expected to be very sensitive to the axial ratio of the ellipsoids (see the article by Hughes and Jain (1979)). We observe a significant variation in the position of the second band. Thus it appears at 3.40 eV in figure 5 and at 3.56 eV in figure 6. This might be expected in view of the different ion species implanted in the two cases. We have annealed a similarly implanted crystal to the one shown in figure 5 in which peak doubling did not occur (Davidson *et al* 1986).

With regard to the main colloid peak located at 520 nm (2.38 eV) in figure 5, its location is not in good agreement with the Doyle theory (1958) for spherical lithium colloids in LiF, which predicts a peak near 385 nm (3.22 eV). As can be seen in table 2, the Doyle equation successfully predicts the band position for a variety of colloids. Calculations by Radchenko (1970) using the Mie equations place the lithium colloid band at 460 nm (2.70 eV) for small particles. A larger particle radius of the order of 30 nm is needed to locate the band at 520 nm. We consistently observe the lithium colloid band near 520 nm in our LiF investigations where we produce intrinsic colloids by implanting rare gas ions.

The occurrence of lithium colloids in irradiated LiF crystals is not well characterized in the literature. Lithium ions have been implanted in LiF by Davenas *et al* (1973) and recently by Alekseeva *et al* (1993). The concentration of implanted lithium ions was on the small side in the former investigation and gave a colloid band at 445 nm (2.79 eV) while the spectra obtained by the latter gave strong absorption peaking at wavelengths in the region of 500–520 nm. This is similar to the spectrum shown in figure 5 observed during the present investigation in crystals implanted with argon ions. In the present case the lithium colloid band has low absorbance since the atoms responsible are derived from the host crystal. We find that the lithium colloid is produced readily in argon-ion-implanted crystals under normal conditions. It is observed less readily in neon-ion-implanted crystals (Davidson *et al* 1986), and we have also produced it in samples implanted with krypton ions. There is thus a fair body of evidence for the presence of lithium colloids in ion-implanted LiF crystals althought the wide range of values and the occasional peak doubling indicate a sensitivity to the microstructure of the radiation damage on the part of the lithium colloid.

4.4. Dislocations

A very significant effect mentioned earlier, which also concerns lithium colloids, is shown in figure 6. We refer to the observation of a lithium colloid in a few crystals implanted with sodium or magnesium ions. In this situation one might have expected the colloid to consist of the implanted ions. An explanation favoured here involves dislocations. These are known to be preferential sites for metal precipitates and the decoration of dislocations is well documented in alkali halides in general and in LiF in particular (Amelinckx 1964, Hobbs *et al* 1974). We think it likely that dislocations enhance the formation of intrinsic colloids by favouring the aggregation of F centres in their vicinity. We have noticed deviant behaviour previously when nominally similar KI crystals doped with Sr and coloured by

γ-rays behaved differently on annealing (Allen 1991). This could be accounted for by the presence of dislocations in one of the samples. If this proposal is correct, the anomalous results reported here are characteristic of the annealing behaviour of dislocation-rich crystals.

Dislocations may be incorporated in crystals during growth, cleavage or polishing and are also introduced into alkali halides by the irradiation process itself. Radiation-induced dislocation loops have been observed using the electron microscope by Hobbs (1975). It is not surprising therefore that their presence might influence annealing experiments. We note that the explanation we offer for the peak-doubling effect requires some preferential alignment or periodicity on the part of the aspherical lithium colloids. This could be provided by dislocations. Hobbs *et al* (1974) in their electron microscopy investigations observed a tendency for colloids to elongate and adopt a regular spacing along dislocation lines. This provides circumstantial support for our suggestion about non-spherical lithium colloids. The present work is the first to associate dislocations with specific features of the optical absorption spectrum of LiF.

In this connection we have noticed a violet colouration in a few pure crystals implanted with magnesium ions. It occurs at high annealing temperatures near 520 °C when the magnesium colloids themselves are disappearing. We note that the bands responsible for the colouration occur at wavelengths attributed earlier to lithium colloids shown in figure 5 and in figure 6. This may be a further indication of lithium atoms in the form of colloids trapped at dislocations.

5. Conclusion

(i) Pure and magnesium-doped LiF crystals have been implanted with mainly Mg^+ and Ar^+ ions at fluences in the range 6×10^{15}–1×10^{17} cm^{-2}.

(ii) Isochronal annealing leads to colloid development with mobile F centres playing an essential role in the process.

(iii) Lithium colloids absorbing near 520 nm form in crystals implanted with Ne^+, Ar^+ and Kr^+ ions. Subsequent thermal annealing may induce a platelet morphology. We report the presence of lithium colloids in a few crystals implanted with Mg^+ and Na^+ ions at fluences of 1×10^{16} cm^{-2}. We suggest that dislocations are responsible for this anomalous annealing behaviour.

(iv) Magnesium colloids absorbing near 280 nm generally form in pure samples implanted with Mg^+ ions.

(v) Magnesium colloids also form when annealing magnesium-doped crystals implanted with rare gas ions. While similarities to a gettering process exist, the responsible mechanism is thought to involve the interaction of F centres with impurity–vacancy dipoles.

Acknowledgments

ATD thanks Professor B Spoelstra for continued interest. Financial support is acknowledged from the Research Committee of the University of Zululand and from the University Development Programme of the Foundation for Research Development (FRD). JDC thanks the FRD for research support.

References

Abu-Hassan L H and Townsend P D 1986 J. Phys. C: Solid State Phys. **19** 99–110
Afonso C N, Ortiz C and Clark G J 1985 *Phys. Status Solidi* b **131** 87–96
Agulló-López F, López F L and Jaque F 1982 *Cryst. Latt. Defects Amorph. Matter.* 9 227–52
Alekseeva L I, Titov Y M, Urusovskaya A A, Knab G G, Guseva M I and Gordeeva G V 1993 *Phys. Status Solidi* b **178** 71–85
Allen A M T 1991 *Doctoral Thesis* Univeristy of the Witwatersrand
Amelinckx S 1964 *The Direct Observation of Dislocations* (New York: Academic)
Beall Fowler W 1968 *Physics of Colour Centres* (New York: Academic)
Comins J D, Davidson A T and Derry T E 1988 *Defect Diffus. Forum* **57/58** 409–24
Crittenden G C, Townsend P D and Townshend S E 1974 *J. Phys. D: Appl. Phys.* 7 2397–409
Davenas J, Perez A, Thevenard P and Dupuy C H S 1973 *Phys. Status Solidi* a **19** 679–86
Davidson A T, Comins J D and Derry T E 1985 *Radiat. Eff.* **90** 213–25
Davidson A T, Comins J D, Derry T E and Khumalo F S 1986 *Radiat. Eff.* **98** 305–12
Davidson A T, Comins J D, Derry T E and Raphuthi A M J 1993 *Phys. Rev.* B **48** 782–8
Doyle W T 1958 *Phys. Rev.* **111** 1067–77
Gray D E 1972 *American Institute of Physics Handbook* 3rd edn (New York: McGraw-Hill) pp 6–34
Hobbs, L W 1975 *Surface and Defect Properties of Solids* vol 4 (London: Chemical Society)
Hobbs L W, Hughes A E and Chassagne G 1974 *Nature* **252** 383–5
Hughes A E and Jain S C 1979 *Adv. Phys.* **28** 717–828
Kittel C 1976 *Introduction to Solid State Physics* 5th edn (New York: Wiley)
Kos H J and Nink R 1977 *Phys. Status Solidi* a **41** K157–K161
—— 1979 *Phys. Status Solidi* a **56** 593–6
Landreth J L and McKeever S W S 1985 *J. Phys. D: Appl. Phys.* **18** 1919–33
Lecrosnier D 1983 *Nucl. Instrum. Methods* **209** 325–32
Mayhugh M R, Christy R W and Johnson N M 1970 *J. Appl. Phys.* **41** 2968–76
McKeever S W S 1985 *Thermoluminescence of Solids* (Cambridge: Cambridge University Press)
Radchenko I S 1970 *Sov. Phys.–Solid State* **11** 1476–9
Shluger A, Mysovsky S and Nepomnyaschikh A 1988 *J. Phys. Chem. Solids* **49** 1043–5
Townsend P D 1987 *Rep. Prog. Phys.* **50** 501–58